JOURNAL OF SPACECRAFT AND ROCKETS
Vol. 47, No. 1, January–February 2010

Engineering Notes

Tether Capture and Momentum Exchange from Hyperbolic Orbits

Paul Williams*
Delft University of Technology,
3104 VIC Delft, The Netherlands

DOI: 10.2514/1.44873

Introduction

TETHERED space systems have been proposed for a wide range of future space applications. These include the deployment of payloads [1], momentum exchange [2,3], and power generation via electrodynamic tethers [4]. One of the most promising applications of tethered space systems is momentum exchange. Arnold [5] demonstrated the basic features of momentum exchange by calculating the altitude gains possible by releasing the end masses from a tether in a circular orbit. For an Earth-pointing tether in equilibrium, the payload can gain an altitude of approximately 7 times the tether length; for a swinging tether the altitude gains vary between 7 and 14 times the tether length, depending on when the payload is released; for a spinning tether, the altitude gains are greater than 14 times the tether length [6]. Extension of momentum exchange to consider rotating tethers in elliptical orbits led to the proposal for systems capable of transferring payloads to Mars and back [2]. The so-called MXER [7] (momentum-exchange electrodynamic reboost) system is the culmination of much of this work, which could be used to boost spacecraft from low-Earth parking orbits to geosynchronous transfer orbits and beyond. The MXER system proposes to regain the lost momentum of the larger body through application of an electrodynamic tether to reboost the orbit of the body.

The reverse process can also be considered for slowing a spacecraft on a hyperbolic trajectory using a tether. The idea, first mentioned by Longuski et al. [8], was developed by Williams et al. [3] who showed that the maneuver was not only physically possible, but that significant mass savings can be accrued through such a system. The maneuver considered in [3] uses a single tether system in a hyperbolic orbit to slow a payload by means of the tether rotational energy. One of the limitations of the approach is that the tether system used to impart momentum must do all of the work. This means that the mass requirements for the tether are not necessarily optimal. If more than one tether system is used, however, then the tether mass can be distributed over more than one tether. This could result in greater savings in mass than a single tether system. In future space activities, it is likely that systems will be placed in permanent orbits around key planets in the solar system. With the assumption of a base tether system at a target planet, the reduction of tether mass for the tether system in the hyperbolic orbit becomes possible by spinning the base tether system to fast enough speeds. By adjusting the properties of the two-tether systems, it may be possible to obtain a family of optimal mass configurations, characterized by the ratio of mass allocated between the two-tether systems. This possibility has not been considered in previous works related to tethered systems, and is the main contribution of this work.

This Note explores the concept which is summarized in Fig. 1. The base tether system is in orbit around the target planet (A). An incoming spacecraft deploys a payload on a tether (B) and controls the motion in such a way that it is spinning at the desired rate (C). The base tether system is also controlled such that the tips of the tethers on both systems rendezvous with zero relative velocity (C). Following rendezvous, the base tether system continues orbiting the target planet, while the system on the hyperbolic orbit gains a boost in velocity due to the momentum exchange. In addition, because the spacecraft performs a flyby of the target planet, the passing spacecraft gains momentum due to gravity-assist. The combined maneuver without the base tether system is termed a Momentum Enhanced Gravity Assist (MEGA) maneuver in [9]. In this Note, the maneuver with a two-tether system is termed a MEGA-2 maneuver. The key contributions of this work are the determination of optimal system configurations that minimize the mass of the tether used in the passing tether system, and the feasibility of using variations in tether length to control the large-scale motion of the tethers in preparation for rendezvous. Unlike previous studies that have focused on systems in Earth orbit [7], this Note presents results for capture at Venus.

Mathematical Model

The MEGA-2 maneuver relies on two-tethered systems. For simplicity, both tether systems are modeled using inextensible, rigid dumbbell models. The dumbbell model has been widely used in studies of tether dynamics and control and is sufficient for studying the initial feasibility of a concept [6]. A representation of the mathematical model of a single tether system and the coordinates used to describe the motion is given in Fig. 2. The center of mass of the system is assumed to be in an orbit described by the radius r and the true anomaly ν. The tether motion is described in the local orbital coordinate frame Oxy, attached to the system center of mass at O. The orientation of the tether system is described by the in-plane tether libration angle θ. The tether length is denoted by l.

The main satellite from which the tether is deployed is $m_1 = m_1^0 - \rho l$, and the subsatellite/payload/capture device is m_2. The tether mass is assumed to be uniform along its length with line density ρ. The total tether mass is given by $m_t = \rho l$.

For convenience, the equations of motion are nondimensionalized. The true anomaly of the passing spacecraft ν_1 is used as the independent variable for both tether systems. The nondimensional equations of motion for the jth tether system are given by [3]

$$\begin{aligned}\theta_j'' &= 2\frac{e_1 \sin\nu_1}{1+e_1\cos\nu_1}\theta_j' + 2\frac{e_j\sin\nu_j}{1+e_j\cos\nu_j}\left(\frac{\dot{\nu}_j}{\dot{\nu}_1}\right)^2 \\ &\quad - 2\left(\theta_j' + \frac{\dot{\nu}_j}{\dot{\nu}_1}\right)\frac{m_1^{(j)}(m_2^{(j)} + \frac{m_t^{(j)}}{2})}{m^{(j)}m^{(j)*}}\frac{\Lambda_j'}{\Lambda_j} \\ &\quad - \frac{3}{1+e_j\cos\nu_j}\left(\frac{\dot{\nu}_j}{\dot{\nu}_1}\right)^2\sin\theta_j\cos\theta_j \end{aligned} \tag{1}$$

$$\begin{aligned}\Lambda_j'' &= \frac{2e_1\sin\nu_1}{1+e_1\cos\nu_1}\Lambda_j' - \frac{(2m_1^{(j)} - m^{(j)})\frac{m_t^{(j)}}{2}}{m_1^{(j)}(m_2^{(j)} + m_t^{(j)})}\frac{\Lambda_j'^2}{\Lambda_j} \\ &\quad + \frac{m_2^{(j)} + \frac{m_t^{(j)}}{2}}{m_2^{(j)} + m_t^{(j)}}\Lambda_j\left[\left(\theta_j' + \frac{\dot{\nu}_j}{\dot{\nu}_1}\right)^2 + \left(\frac{\dot{\nu}_j}{\dot{\nu}_1}\right)^2\left(\frac{3\cos^2\theta_j - 1}{1+e_j\cos\nu_j}\right)\right] \\ &\quad - \frac{T_j}{m_1^{(j)}\dot{\nu}_1^2(m_2^{(j)} + m_t^{(j)})L_j/m^{(j)}}\end{aligned} \tag{2}$$

Received 11 April 2009; revision received 22 September 2009; accepted for publication 22 September 2009.

*Applied Researcher, Faculty of Aerospace Engineering, 1/4 Maylands Avenue, Balwyn North. AIAA Member.

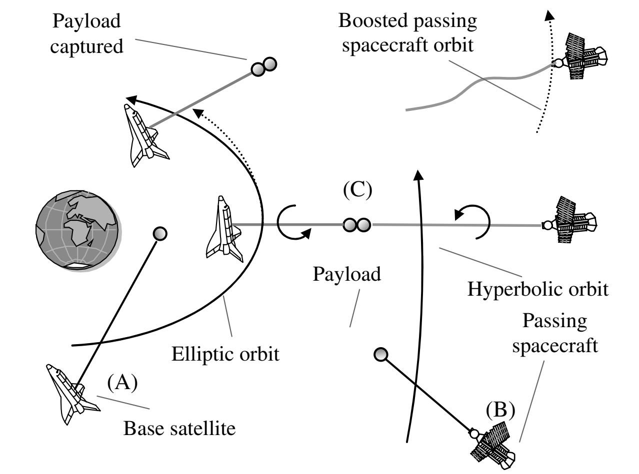

Fig. 1 Momentum Enhanced Gravity Assist-2 (MEGA-2) maneuver for delivery and capture of payloads.

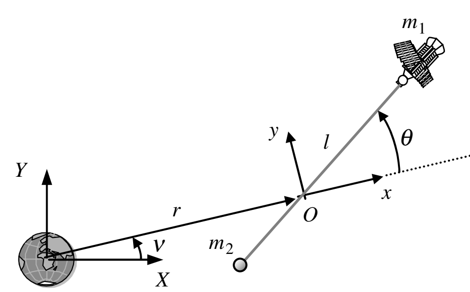

Fig. 2 In-plane tether dumbbell model.

where e_j is the orbit eccentricity of the jth tether system, $\Lambda_j = l_j/L_j$, L_j is a reference tether length, T_j is the jth tether tension, and $()' = \mathrm{d}()/\mathrm{d}\nu_1$.

These equations depend on ν_2, for which an additional differential equation is required:

$$\nu_2' = \dot{\nu}_2/\dot{\nu}_1 \tag{3}$$

In this section, the tether states are related to the instantaneous position and velocity of the tether end bodies. This knowledge is used to derive the necessary conditions for zero relative position, zero relative velocity rendezvous. It is assumed that both tether systems are in coplanar orbits and are rotating in the orbital plane. Referring to Fig. 2, the inertial positions of the tips of the tether k are obtained as

$$\begin{aligned} X_1^{(k)} &= (r_k + s_1^{(k)} \cos\theta_k)\cos\nu_k - s_1^{(k)}\sin\theta_k \sin\nu_k \\ Y_1^{(k)} &= s_1^{(k)}\sin\theta_k\cos\nu_k + (r_k + s_1^{(k)}\cos\theta_k)\sin\nu_k \end{aligned} \tag{4}$$

$$\begin{aligned} X_2^{(k)} &= (r_k - s_2^{(k)} \cos\theta_k)\cos\nu_k + s_2^{(k)}\sin\theta_k \sin\nu_k \\ Y_2^{(k)} &= -s_2^{(k)}\sin\theta_k\cos\nu_k + (r_k - s_2^{(k)}\cos\theta_k)\sin\nu_k \end{aligned} \tag{5}$$

where $s_1^{(k)} = (m_2^{(k)} + m_t^{(k)}/2)l^{(k)}/m^{(k)}$ and $s_2^{(k)} = (m_1^{(k)} + m_t^{(k)}/2)l^{(k)}/m^{(k)}$. The inertial velocities of the tips of the tethers are obtained by taking the time derivatives of Eqs. (4) and (5). For the sake of brevity, these are omitted here. To ensure a gentle rendezvous, the following conditions should be met:

$$X_2^{(1)} = X_2^{(2)}, \qquad Y_2^{(1)} = Y_2^{(2)} \qquad \dot{X}_2^{(1)} = \dot{X}_2^{(2)}, \qquad \dot{Y}_2^{(1)} = \dot{Y}_2^{(2)} \tag{6}$$

In this development, it has been assumed that the two-tether systems are coplanar. The tether length rate at capture is assumed to be zero, and the two systems are assumed to share a common argument of periapsis, with rendezvous occurring at $\nu_1 = \nu_2 = 0$. The orientation of the tethers at rendezvous are prescribed to be $\theta_1 = 0$, $\theta_2 = \pi$, which assumes the flyby orbit is higher than the base system. Furthermore, because capture is prescribed to occur at periapsis for both systems, it is easy to verify that the radial components of the relative velocity are zero at the instant of capture. Matching of the tangential components of velocity leads to a required nondimensional spin rate of the flyby system at capture of

$$\theta_1' = \frac{r_1}{s_2^{(1)}} - 1 - (r_2 + s_2^{(2)} + s_2^{(2)}\tilde{\theta}_2')\frac{\dot{\nu}_2}{s_2^{(1)}\dot{\nu}_1} \tag{7}$$

where the nondimensional spin rate of the base satellite is used as a parameter $\tilde{\theta}_2' = \dot{\theta}_2/\dot{\nu}_2$.

Mass Requirements for Spinning Rendezvous

Simulation of the dynamics of a particular rendezvous maneuver generates a tension time history that includes the effects of the forces induced by the tether rotation as well as the tension induced by the gravity-gradient. Tension can be calculated using Eq. (2) by substituting $\Lambda_j'' = \Lambda_j' = 0$. The tension is important for characterizing a particular maneuver from two perspectives: 1) the tension must be greater than zero for the system motion to be controllable via tension/length control, 2) the tension must not be too large so as to cause failure of the tether material. Both of these issues are addressed via an iterative design methodology.

The procedure used to derive the mass requirements for a particular configuration is as follows: first, the orbit eccentricity of the passing spacecraft, e_1, the orbit eccentricity of the base tether system, e_2, the tether lengths L_1 and L_2, the tether densities ρ_1 and ρ_2, the end masses of the tethered systems $m_1^{(k)}$ and $m_2^{(k)}$, $k = 1, 2$, and the nondimensional spin rate of the base tether system, θ_2', are specified. The radius to periapsis of the base satellite at capture is fixed, r_1. Using this information, the radius to periapsis and semimajor axis of the passing satellite are calculated for a radially-aligned capture. The required nondimensional spin rate of the passing tether system is calculated from Eq. (7). The equations of motion are integrated backwards from the rendezvous point to $\nu_1 = 0.1745 - \cos^{-1}(-1/e_1)$, i.e., 10 deg less than the asymptote of the hyperbolic orbit.

Tether Mass

Assume that the initial tether line density has been specified as $(\rho_k)_0 = \bar{\rho}A_k$, $k = 1, 2$, where $\bar{\rho}$ is the tether mass density, and A_k is the cross-sectional area of the tether. Following a simulation of the system, the maximum and minimum tether tension are recorded:

$$T_{\max}^k = \max(T_k), \qquad T_{\min}^k = \min(T_k) \tag{8}$$

The maximum tension is used to determine the required cross-sectional area of the tether based on the design stress σ_d and factor of safety F:

$$A_k = FT_{\max}^k/\sigma_d \tag{9}$$

If the new line density based on A_k is within a prescribed tolerance of the previous value

$$|(\bar{\rho}A_k)_j - (\rho_k)_{j-1}| < \mathrm{tol} \tag{10}$$

then the iteration is terminated after n iterations and convergence is declared. Since the cross-sectional is constant along the tether, the jth tether mass is obtained simply as $\bar{\rho}A_n L_j$.

Optimization of System Parameters

By systematically varying the spin rate of the base system at capture, the eccentricity of the base tether system, as well as the tether lengths, it is possible to build maps of the required tether mass. However, these become time consuming to generate for cases in which more than two variables are varied. An alternative approach is to use an optimization approach that directly determines the combination of variables that minimizes a selected performance index, such as tether mass. This is the approach taken in this Note. A global optimization strategy has been selected because of the highly nonlinear and chaotic behavior of the system dynamics, which can lead to problems with convergence for gradient-based algorithms. Simulated annealing [10] was selected as the optimization approach.

The problem of determining optimal MEGA-2 configurations is posed as follows: find the optimal solution vector $\boldsymbol{x} := \{e_2, \theta_2', l_1, l_2\}$ that minimizes the cost function

$$J = (1 + e_2)(\alpha m_t^{(1)} + m_t^{(2)}) + J_p \tag{11}$$

where J_p is a penalty function defined as a function of the minimum tension

$$J_p := \begin{cases} 10^6 & T_{\min}^1 \leq 0 \text{ or } T_{\min}^2 \leq 0 \\ 0 & T_{\min}^1 > 0 \text{ and } T_{\min}^2 > 0 \end{cases} \tag{12}$$

and α is a constant weighting factor that measures the importance of minimizing the passing system's tether mass over the base tether system mass.

Guidance Approach for Rendezvous

One of the biggest challenges with the proposed system is the need to rendezvous the tips of two-tether systems. Detailed design must consider the problem of cooperative control in the final stages of rendezvous. However, for the purposes of this work, focus is on controlling the large-scale motion of the tether to correct for large initial pointing errors and random disturbances during the approach phase. Each of the tether systems are assumed to be controlled independently for this analysis.

The guidance approach involves generating completely new optimal trajectories online from the tether system's current position until the rendezvous point. This approach has also been studied for tethered satellite systems during retrieval [11], as well as reentry trajectories of space vehicles [12]. This type of approach works best for systems that may be subjected to initial errors, and can become dangerous for systems with the possibility of large disturbances. This is because of the fact that the system is being guided towards a fixed state at a fixed time. Large disturbances near the final time would make the control problem infeasible. It should be noted that in such a circumstance, if the optimal maneuver has no feasible solution, then no controller would be able to generate a control signal to ensure rendezvous.

The control problem is posed as: find the optimal variation in the tether reel acceleration $\ddot{l}_j$ that minimizes the cost function

$$J_c = \int_{\nu_0}^{0} (\ddot{l}_j)^2 \mathrm{d}\nu \tag{13}$$

subject to the dynamic constraints given by Eqs. (1) and (2), as well as the tension constraints

$$T_j > 0, \qquad j = 1, 2 \tag{14}$$

and the box constraints on the nondimensional tether length

$$0.5 \leq \Lambda_j \leq 1.5, \qquad j = 1, 2 \tag{15}$$

The control problem is completed by specifying the initial conditions constraints

$$\theta(\nu) = \theta_\nu, \quad \theta'(\nu) = \theta_\nu', \quad \Lambda(\nu) = \Lambda_\nu, \quad \Lambda'(\nu) = \Lambda_\nu' \tag{16}$$

for each tether, as well as the terminal constraints

$$\theta(0) = \theta_f, \quad \theta'(0) = \theta_f', \quad \Lambda(0) = \Lambda_f, \quad \Lambda'(0) = \Lambda_f' \tag{17}$$

for each tether, which are derived from the rendezvous requirements presented in the previous sections. The nominal initial conditions constraints are derived based on the time propagation of the tether dynamic states from rendezvous to the initial time. Monte Carlo simulations of the closed-loop controller are conducted by perturbing the nominal initial conditions.

Note that the control variable is selected as the dimensional reel acceleration rather than the nondimensional one. This is because of the large changes in the nondimensional variables for tether systems in hyperbolic and elliptical orbits with large eccentricities. A simple transformation of variables is used to implement the control signal in the numerical simulations. The control is bounded by the following constraint:

$$-5 \leq \ddot{l}_j \leq 5 \text{ m/s}^2 \tag{18}$$

It is important to realize that the above problem is essentially open-loop. However, the loop can be closed by providing sampled-data feedback of the tether state at regular sampling intervals and resolving the same problem from the sample time. Implementation of the closed-loop controller is achieved by way of the Legendre pseudospectral method [13–15]. The closed-loop simulations are conducted using MATLAB with Gaussian noise applied to the simulated librational dynamics. The process noise is defined in the following manner:

$$\theta_j'' = f_\theta(\theta_j, \theta_j', \Lambda_j, \Lambda_j') + \frac{w_\theta}{\dot{\nu}_1^2} \tag{19}$$

where w_θ represents the process noise with zero mean and covariance Q_θ. Note that the scaling of the noise with the inverse of the square of the orbital angular velocity is due to the nondimensionalization of the libration equation.

Numerical Results

The iterative design technique described above was implemented for the MEGA-2 system at Venus. In order to keep the amount of computation to a minimum, the hyperbolic orbit eccentricity is held constant at 1.15. The other key parameters that are held fixed are given in Table 1. All integrations are carried out with the equations of motion implemented in a C++ mex-file (MATLAB compiled executable) using the LSODA variable-step integrator. Absolute and relative tolerances of 10^{-9} are used to control the integration errors.

Optimal System Configurations

Optimal configurations for the tether systems were determined by fixing the eccentricity of the base tether system at $e_2 = 0.95$. To ensure that the solution converges to the global minimum, the optimization is run several times from different initial guesses. Results of the optimizations for α varied between 1 and 10 and are shown in Table 2. By way of comparison, the propellant mass required to decelerate the 200 kg payload from the hyperbolic orbit to a parabolic (on the verge of being captured) orbit can be calculated from

$$v_\infty^2 = \mu(e_1 - 1)/r_1 \tag{20}$$

Table 1 Parameters used for MEGA-2 at Venus

Parameter	Value
Gravitational parameter, μ	3.25×10^{14} m^3/s^2
Periapsis radius, r_p	7000 km
Eccentricity of hyperbolic orbit, e_1	1.15
Mass of passing system, $m_1^{(1)}$	2000 kg
Payload mass, $m_2^{(1)}$	200 kg
Mass of base tether system, $m_1^{(2)}$	10000 kg
Subsatellite/capturing mechanism mass, $m_2^{(2)}$	1000 kg
Mass density of tether material, $\bar{\rho}$	970 kg/m^3
Factor of safety, F	1.5
Design strength, σ_d	4 GPa

Table 2 Optimized MEGA-2 configurations at Venus

α	$m_t^{(1)}$, kg	$m_t^{(2)}$, kg	m_{total}, kg	θ_2'	l_1, km	l_2, km
1	10.01	2.14	12.15	0.96	135.27	26.77
2	6.51	7.61	14.12	1.14	126.53	47.12
3	5.60	9.95	15.55	0.98	101.90	57.49
4	4.72	13.50	18.22	0.24	93.89	92.83
5	3.63	17.93	21.57	0.99	81.43	76.50
6	3.35	20.23	23.58	2.64	77.81	47.90
7	2.56	24.29	26.85	0.96	68.29	89.88
8	2.20	27.00	29.20	0.99	63.22	93.55
9	1.91	29.47	31.38	0.83	59.01	104.35
10	1.67	31.70	33.37	0.99	55.10	101.13

$$\Delta v = \sqrt{\frac{2\mu}{r_1} + v_\infty^2} - \sqrt{\frac{2\mu}{r_1}} \tag{21}$$

$$m_{\text{prop}} = m_2^{(1)}(e^{\frac{\Delta v}{I_{\text{sp}} g}} - 1) \tag{22}$$

where I_{sp} is the specific impulse of the rocket motor, and $g = 9.81\ \text{m/s}^2$ is the gravitational acceleration at Earth sea-level. The propellant mass is approximately 25 kg for the parameters used in these examples with a specific impulse of 300 sec.

The optimal total mass configuration ($\alpha = 1$) results in a total tether mass of 12.15 kg, roughly half the propellant required. The tether lengths are quite disparate with the passing tether system length 5 times the base tether system length for $\alpha = 1$. As the weighting factor on the mass of tether 1 is increased, the total tether mass increases. The results show that the length of tether 1 decreases with a corresponding increase in the length of tether 2 as the weighting on the mass of tether 1 becomes more important. For roughly the same amount of total tether mass across the two systems as propellant mass, one could design the two tethers such that tether 1 has a mass of only 1.67 kg for $\alpha = 10$. Hence, through reuse of tether 2, fifteen 200 kg payloads could be captured from hyperbolic orbits for the cost of one propellant capture. Another feature of the results is that the optimal spin rate of the base tether system is unpredictable as the weighting parameter changes.

Optimal Control of Spinning Rendezvous

The feasibility of the MEGA-2 maneuver has been established from the point of view of dynamics in the previous sections. This means that it is not only possible, but it is advantageous to use the maneuver as described. Up until this point, it has been assumed that the system is spinning perfectly at the desired rate and is at the desired orientation(s) prior to the rendezvous event. However, it is not clear how sensitive any particular maneuver is to timing nor whether the system(s) can be controlled in the case of disturbances or initial alignment errors. These issues are considered in this section.

A MEGA-2 maneuver was selected from Table 2 corresponding to $\alpha = 3$. The closed-loop response is obtained with the control problem discretized using 30 nodes. The sample rate is measured in terms of the nondimensional time and is fixed at 0.01 rad. Higher update rates are possible, but not considered in this Note. Initial errors were applied randomly with standard deviations of 1 rad on the initial orientation, and 30 on the nondimensional spin rate. A white process noise with standard deviation of 10^{-5} is applied to the libration dynamics so that continual corrections are required by the controller. During closed-loop simulation, each solution is used as the initial guess for the subsequent computation of the optimal trajectory. Only results from the passing tether system are shown in this Note.

Numerical results for the passing tether system are shown in Figs. 3 and 4 for 50 simulations. In all of the simulations, the final constraints are met to less than the prescribed tolerance of 10^{-6}. Figure 3 shows the reeling dynamics of the tether. The results show that, in general, most of the control work is done at true anomalies between $-2 \leq \nu_1 \leq -1.5$ rad, as opposed to earlier in the maneuver

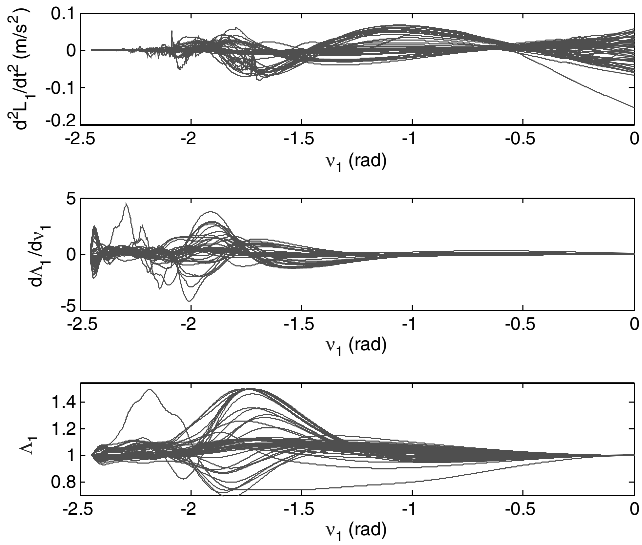

Fig. 3 Optimal closed-loop reeling dynamics with initial libration errors and Gaussian white noise on librational dynamics.

(with the exception of one case). Reeling earlier does not alter the librational dynamics significantly due to the lower Coriolis forces on the system. Figure 4 shows the libration response of the system during closed-loop simulations. It is evident from these plots that the librations converge to zero error at the terminal time. Note, however, that the controller is not designed to minimize deviations from the reference trajectory, but to meet the terminal constraints with the least amount of tether reeling. The required reeling acceleration, shown in Fig. 3, is very moderate ($<0.1\ \text{m/s}^2$). Figure 4 highlights the exception case in the reeling dynamics, where the initial libration error is approximately 180 deg. The results show that this solution is possibly a local minimum; that is, the final angle is 0, as opposed to a multiple of 2π. This is caused by the fact that the reference trajectory is used as an initial guess.

The numerical results of the closed-loop controller demonstrate that the proposed maneuver is feasible from a dynamics and control point of view. All control authority to achieve a high precision rendezvous has been achieved by simply changing the tether length. No propellant is necessary to realize the control, which makes the system even more attractive. However, the results are achieved under the assumption that the orbits remain unperturbed and the tethers are inelastic. Further work should be undertaken to assess the orbit

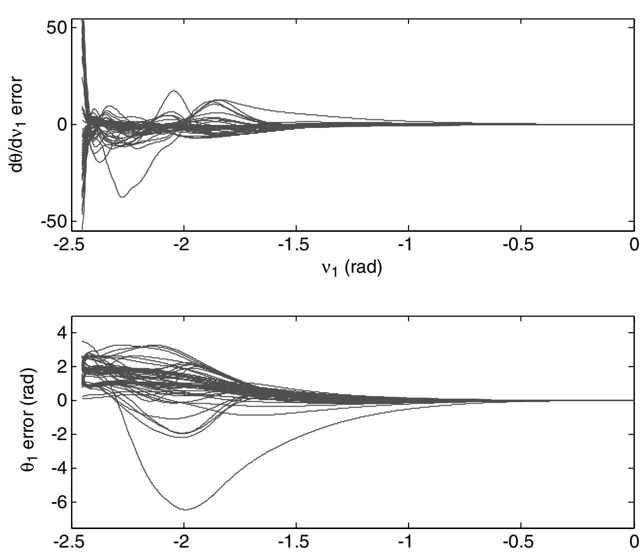

Fig. 4 Optimal closed-loop libration dynamics with initial libration errors and Gaussian white noise on librational dynamics.

control requirements that would be necessary to achieve such high precision rendezvous.

Conclusions

The dynamics and control of a tether-assisted rendezvous and capture maneuver from a hyperbolic orbit have been investigated using a dual tether system. The maneuver offers advantages over a conventional propellant maneuver, or a similar maneuver using a single rotating tether. The advantage comes from being able to reuse the tether mass that remains in orbit at the target planet. Based on an iterative design technique using actual physics models, a 50% savings in propellant can be achieved for a comparable fuel-burn capture maneuver performed at Venus. By trading the mass of the passing tether for mass of the base tether system, mass savings on the order of 90% for the disposable tether can be achieved compared to a conventional propellant maneuver. One of the additional challenges of using a dual tether system compared to a single tether system is the need for closed-loop control. Using simulation models with large initial pointing errors and process noise, it is possible to control the tether orientation and velocity using manipulation of the tether length alone. Because the power for such manipulation of length could come from solar panels, it is evident that the proposed maneuver could potentially be used for performing propellantless planetary capture.

References

[1] Carroll, J. A., "Tether Applications in Space Transportation," *Acta Astronautica*, Vol. 13, No. 4, 1986, 1984, pp. 165–174. doi:10.1016/0094-5765(86)90061-5

[2] Nordley, G. D., and Forward, R. L., "Mars–Earth Rapid Interplanetary Tether Transport (MERITT) System: Initial Feasibility Analysis," *Journal of Propulsion and Power*, Vol. 17, No. 3, 2001, pp. 499–507. 10.2514/2.5798.

[3] Williams, P., Blanksby, C., and Trivailo, P., "Tethered Planetary Capture Maneuvers," *Journal of Spacecraft and Rockets*, Vol. 41, No. 4, 2004, pp. 603–613. doi:10.2514/1.1024

[4] Gallagher, D. L., Johnson, L., Moore, J., and Bagenal, F., "Electrodynamic Tether Propulsion and Power Generation at Jupiter," NASA Marshall Space Flight Center, NASA/TP-1998-208475, June 1998.

[5] Arnold, D. A., "The Behavior of Long Tethers in Space," *The Journal of the Astronautical Sciences*, Vol. 35, No. 1, 1987, pp. 3–18.

[6] Bekey, I., and Penzo, P. A., "Tether Propulsion," *Aerospace America*, Vol. 24, July 1986, pp. 40–43.

[7] Sorensen, K. F., "Conceptual Design and Analysis of an MXER Tether Boost Station," 37th AIAA/ASME/SAE/ASEE Joint Propulsion Confer- ence and Exhibit, Salt Lake City, UT, AIAA Paper 2001-3915, 8–11 July 2001.

[8] Longuski, J. M., Puig-Suari, J., and Mechalas, J., "Aerobraking Tethers for the Exploration of the Solar System," *Acta Astronautica*, Vol. 35, No. 2/3, 1995, pp. 205–214. doi:10.1016/0094-5765(94)00273-O

[9] Williams, P., Blanksby, C., and Trivailo, P., "Tethered Planetary Capture: Controlled Maneuvers," *Acta Astronautica*, Vol. 53, Nos. 4–10, 2003, pp. 681–708. doi:10.1016/S0094-5765(03)80029-2

[10] Press, W. H., Teukolsky, S. A., Vetterling, W. T., and Flannery, B. P., *Numerical Recipes in* C + +*: The Art of Scientific Computing*, 2nd ed., Cambridge Univ. Press, Cambridge, England, U.K., 2002.

[11] Williams, P., "Real-Time Computation of Optimal Trajectories for Tethered Satellite Systems," AAS/AIAA Astrodynamics Specialist Conference, American Astronautical Society, Paper 05-320, 7–11 Aug. 2005.

[12] Doman, D., Bollino, K. P., and Ross, I. M., "Nonlinear Feedback Control for Rapid, On-Line Trajectory Optimization of Reentry Vehicles," U.S. Air Force Research Lab. Rept. VA-WP-TP-2006-307, Dec. 2005.

[13] Elnagar, G., Kazemi, M. A., and Razzaghi, M., "The Pseudospectral Legendre Method for Discretizing Optimal Control Problems," *IEEE Transactions on Automatic Control*, Vol. 40, No. 10, 1995, pp. 1793–1796. doi:10.1109/9.467672

[14] Ross, I. M., and Fahroo, F., "Legendre Pseudospectral Approximations of Optimal Control Problems," *Lecture Notes in Control and Information Sciences*, Vol. 295, Springer–Verlag, New York, 2003, pp. 327–342.

[15] Williams, P., "Application of Pseudospectral Methods for Receding Horizon Control," *Journal of Guidance, Control, and Dynamics*, Vol. 27, No. 2, 2004, pp. 310–314. doi:10.2514/1.5118

D. Spencer
Associate Editor